

Thermophysical Properties and Water Saturation of [PF₆]-Based Ionic Liquids

Catarina M. S. S. Neves,[†] Marta L. S. Batista,[†] Ana Filipa M. Cláudio,[†] Luís M. N. B. F. Santos,[‡] Isabel M. Marrucho,^{†,§} Mara G. Freire,[†] and João A. P. Coutinho^{*,†}

CICECO, Departamento de Química, Universidade de Aveiro, 3810-193 Aveiro, Portugal, CIQ, Departamento de Química e Bioquímica, Faculdade de Ciências da Universidade do Porto, R. Campo Alegre 687, 4169-007, Porto, Portugal, and Instituto de Tecnologia Química e Biológica, Universidade Nova de Lisboa, Av. República, Apartado 127, 2780-901 Oeiras, Portugal

In this work, mutual solubilities of two [PF₆]-based ionic liquids (ILs) with water and their thermophysical properties, namely, melting properties of pure ILs and densities and viscosities of both pure and water-saturated ILs, were determined. The selected ILs comprise 1-methyl-3-propylimidazolium and 1-methyl-3-propylpyridinium cations combined with the anion hexafluorophosphate. Mutual solubilities with water were measured in the temperature range from (288.15 to 318.15) K. From the experimental solubility data dependence on temperature, the molar thermodynamic functions of solution, such as Gibbs energy, enthalpy, and entropy of the ILs in water were further derived. In addition, a simulation study based on the COSMO-RS methodology was carried out. For both pure ILs and water-equilibrated samples, densities and viscosities were determined in the temperature interval between (303.15 and 373.15) K. The isobaric thermal expansion coefficients for pure and water-saturated ILs were calculated based on the density dependence on temperature.

Introduction

Nowadays, solvent extraction methods are widely used in process engineering, biotechnology, analytical chemistry, and drug production as a way of recovering added-value products from natural sources or for the preconcentration of the samples for an adequate application of quantification techniques. In general, biphasic extraction methods are based on the contact of two immiscible liquid phases or solid/gas–liquid type phases using a suitable solvent for product extraction. A large number of organic solvents can be used for this purpose, their main disadvantages being their toxicity and relatively high volatility and flammability. In this field, ionic liquids (ILs) appear as high-performance and greener solvents, displaying enhanced extraction abilities, minimizing solvent waste, reducing the exposure to hazardous vapors, and generally presenting lower toxicities.^{1,2}

ILs are ionic compounds that belong to the molten salts group and are formed by large organic cations and organic or inorganic anions. The low symmetry, high vibrational freedom, and charge delocalization of the ions composing an IL reduce the stability of the crystalline phases and thus their melting temperatures. Their inherent ionic nature leads to distinctive properties, at least for most of them, such as negligible vapor pressures at room temperature, high thermal stabilities (for instance, decomposition temperatures above 653.15 K for [PF₆]-based ILs),^{3–5} large electrochemical windows, high ionic conductivities, high heat capacities, low flammabilities, and high solvating abilities for organic, inorganic, and organometallic compounds.⁶ Furthermore, the huge number of possible combinations between cations and anions permits the tuning of ILs, allowing them to be designed for a particular application or to show a specific set of intrinsic properties, and thus they are commonly described as “designer solvents”.⁷

Depending on the IL nature, ILs can form biphasic systems with water, organic solvents, solids, or gases, and hence they are suitable for use in liquid–liquid, solid–liquid, and gas–liquid extractions. Indeed, ILs have shown to be useful in the extraction of benzene derivatives,⁸ short chain aliphatic carboxylic acids,⁹ phenol and phenol derivatives,^{10–12} amino acids,^{13,14} antibiotics,¹⁵ azo and acid dyes,^{16,17} and tetrahydrofuran¹⁸ from aqueous systems.

Concerning the studies of the IL extraction ability, one important issue, for which the available information is not sufficient for design purposes, is the mutual solubility of systems involving ILs and the phase containing the product of interest for extraction. Water as the biphasic extraction media plays an important role, and only few publications reporting liquid–liquid equilibria values are available.^{5,19–31} The COSMO-RS, Conductor-like Screening Model for Real Solvents, is a method that predicts the thermophysical properties of fluids making use of unimolecular quantum calculations.^{32–36} There are some previous studies with COSMO-RS applied to the liquid–liquid equilibrium (LLE) description of ILs and alcohols, hydrocarbons, ethers, ketones, and water systems.^{25,27,28,37–43} Unlike other methods such as group-contribution methods (GCMs), equations of state (EoS), and quantitative structure–property relationships (QSPR), this model can be highly valuable in the prediction of solution behavior of systems involving ILs never previously studied and for which other models are not applicable. Taking into account the large number of possible ILs, and additionally their combination with molecular solvents, the use of a predictive method without the need of a priori experimental data could be of main importance in the screening of adequate ILs.

Regarding extraction processes, the IL physical properties of interest are densities, viscosities, and vapor pressures. The lack of significant vapor pressures over wide temperature ranges is one of the outstanding characteristics of ILs that contribute for their “green” status. On the other hand, the density of most ILs is typically greater than water allowing for an easy phase

* Corresponding author. Tel.: +351-234-370200. Fax: +351-234-370084. E-mail: jcoutinho@ua.pt.

[†] Universidade de Aveiro.

[‡] Faculdade de Ciências da Universidade do Porto.

[§] Universidade Nova de Lisboa.

separation by gravity settling.^{44,45} One important feature of ILs regarding extraction processes is their viscosities, since high viscosities restrict mass transfer and increase pumping costs. The strong effect of water upon the viscosity of ILs is important and should be taken into account in the design of extraction processes.⁴⁶

In this work, studies of the mutual solubilities between ILs and water from (288.15 to 318.15) K and of the densities and viscosities of both pure and water-saturated ILs, at \approx (300 \pm 1) K, in the temperature range between (303.15 and 363.15) K and at atmospheric pressure, were carried out. The selected ILs are based on the imidazolium and pyridinium cations combined with the hexafluorophosphate anion. The main goal of this study is to establish the effect of the IL cation family and the water content on their thermophysical behavior.

Experimental Section

Materials. Mutual solubilities with water, densities, and viscosities were studied for the two following ILs: 1-methyl-3-propylimidazolium hexafluorophosphate, [C₃mim][PF₆], and 1-methyl-3-propylpyridinium hexafluorophosphate, [C₃mpy][PF₆]. Both ILs were acquired at Iolitec. To reduce the water and volatile compound content to negligible values, IL individual samples were dried by heating (\approx 353 K), under constant stirring, and at moderate vacuum (\approx 0.1 Pa) for a minimum of 48 h. After this procedure, the purity of the ILs was further checked by ¹H, ¹³C, and ¹⁹F NMR and showed > 99 wt %. The halide mass fraction was found to be < 1 \cdot 10⁻⁴. For the determination of the thermophysical properties of pure or dried ILs, the water mass fraction was determined using a Metrohm 831 Karl Fischer coulometer. The water mass fraction content in the pure ILs for density and viscosity measurements was as follows (measurements carried out before and after measurements in brackets): [C₃mim][PF₆] with [78.75 and 79.63] \cdot 10⁻⁶; [C₃mpy][PF₆] with [54.78 and 56.23] \cdot 10⁻⁶. For mutual solubility studies and determination of the thermophysical properties of water-saturated ILs, the water used was double distilled, passed by a reverse osmosis system, and further treated with a Milli-Q plus 185 water purification apparatus. It has a resistivity of 18.2 M Ω \cdot cm and a TOC (Total Organic Carbon content) smaller than 5 μ g \cdot dm⁻³. The analyte used for the coulometric Karl Fischer titration was Hydranal-Coulomat AG from Riedel-de Haën.

Experimental Procedure. ILs [C₃mim][PF₆] and [C₃mpy][PF₆] are not liquid at room temperature, and their melting temperatures were determined using a Diamond Differential Scanning Calorimetry (DSC) PerkinElmer equipment. The samples were tightly sealed in aluminum pans. The temperature scans were of 0.167 K \cdot s⁻¹ for the temperature range between (278.15 and 323.15) K.

The mutual solubility measurements between water and ILs were carried out at temperatures from (288.15 to 318.15) K and at atmospheric pressure. Due to the high melting temperatures of [C₃mpy][PF₆] and [C₃mim][PF₆], the solubility of water in these ILs was only measured in their liquid state. Note, however, that the presence of water decreases their melting temperatures down to a eutectic point allowing measurements at temperatures below the IL pure state melting temperatures. The IL and the water phases were initially vigorously agitated and allowed to reach saturation equilibrium and complete phase separation, for at least 48 h. This period proved to be the minimum time required to guarantee a complete separation of the two phases and that no further variations in mole fraction solubilities occurred. The temperature was maintained by keeping the glass

vials containing the phases in equilibrium inside an aluminum block specially designed for this purpose, which is placed in an isolated air bath capable of maintaining the temperature within \pm 0.01 K. The temperature control was achieved with a PID temperature controller driven by a calibrated Pt100 (class 1/10) temperature sensor inserted in the aluminum block. To reach temperatures below room temperature, a Julabo circulator, model F25-HD, was coupled to the overall oven system allowing the passage of a thermostated fluid flux around the aluminum block. The solubility of water in the IL-rich phase was determined using a Metrohm 831 Karl Fischer (KF) coulometer, and the solubility of ILs in the water-rich phase was determined by UV-spectroscopy using a SHIMADZU UV-1700 Pharma-Spec Spectrometer, at a wavelength of 211 nm for [C₃mim][PF₆] and 266 nm for [C₃mpy][PF₆], using calibration curves previously established (see detailed description in Supporting Information). These were found to be the maximum UV absorption wavelengths for the imidazolium-based and pyridinium-based cations studied. Both phases were sampled at each temperature from the equilibrium vials using glass syringes maintained dry and at the same temperature of the measurements. For the IL-rich phase, samples of \approx 0.1 g were taken and directly injected in the KF coulometric titrator. For the water-rich phase, samples of \approx 0.5 g were taken and diluted from (250 to 500) cm⁻³ in ultra pure water. The mutual solubility results are an average of at least five independent measurements at each temperature.

Measurements of viscosity and density were performed using an automated SVM 3000 Anton Paar rotational Stabinger viscometer-densimeter. It should be remarked that since both ILs are solid at room temperature viscosities and densities for pure ILs were only determined above their melting temperatures. The SVM 3000 Anton Paar rotational Stabinger viscometer-densimeter uses Peltier elements for fast and efficient thermostatisation. Further details regarding the operation system can be found elsewhere.⁴⁶ No comparison with literature values was made due to the absence of density and viscosity values for the ILs studied in this work. Nevertheless, the equipment was already validated in a previous work⁴⁴ that showed that the experimental data obtained were in good agreement with the literature.^{47,48} The uncertainty in temperature is within \pm 0.02 K. The relative uncertainty in the dynamic viscosity is \pm 0.35 %, while the absolute uncertainty in density is \pm 5 \cdot 10⁻⁴ g \cdot cm⁻³. For dried ILs, measurements were carried out in the temperature range from (318.15 to 363.15) K and at \approx 0.1 MPa. For saturated ILs with water at \approx 300 K, measurements were performed in the temperature interval from (303.15 to 363.15) K. The saturation of each IL with water was attained by vigorously agitating both phases and further allowing the equilibrium for at least 48 h. The mole fraction water content of the water-saturated ILs used in density and viscosity measurements are (0.306 \pm 0.004) and (0.249 \pm 0.006) for [C₃mim][PF₆] and [C₃mpy][PF₆], respectively—values that correspond to the IL–water mutual saturation for a temperature of \approx 300 K.

Though it was shown in a previous work by us³¹ that the [PF₆]⁻ anion was not water stable under specific conditions, the degradation under the conditions used in this work is indeed negligible. The water + IL mutual solubilities were measured at temperatures for which no significant degradation was observed, while the viscosities and densities were measured in very short time periods.

COSMO-RS Calculations. The COSMO-RS calculations were performed at the BP/TZVP level (Turbomole,^{49,50} DFT/COSMO calculation with the BP functional and TZVP⁵¹ basis

Table 1. Experimental Mole Fraction Solubility of Water in ILs, x_w , and of ILs in Water, x_{IL} , as a Function of Temperature and at 0.1 MPa

T/K	$x_w \pm \sigma^a$		$10^3 (x_{IL} \pm \sigma^a)$	
	[C ₃ mim][PF ₆]	[C ₃ mpy][PF ₆]	[C ₃ mim][PF ₆]	[C ₃ mpy][PF ₆]
288.15	0.2437 ± 0.0016	---	1.158 ± 0.040	0.918 ± 0.050
293.15	0.2709 ± 0.0009	---	1.543 ± 0.008	1.223 ± 0.024
298.15	0.2925 ± 0.0009	---	1.957 ± 0.011	1.646 ± 0.029
303.15	0.3168 ± 0.0025	0.2949 ± 0.0020	2.528 ± 0.012	1.990 ± 0.002
308.15	0.3461 ± 0.0003	0.3248 ± 0.0008	2.772 ± 0.066	2.204 ± 0.028
313.15	0.3769 ± 0.0029	0.3516 ± 0.0035	2.965 ± 0.021	2.363 ± 0.020
318.15	0.4050 ± 0.0017	0.3772 ± 0.0025	3.314 ± 0.015	2.689 ± 0.027

^a Standard deviation.

set using the optimized geometries at the same level of theory) with the parameter files BP_TZVP_C2.1_0110 and BP_TZVP_C2.1_0105. The calculations were made for a ternary mixture where the cation and anion were treated as isolated species at equimolar conditions.

Results and Discussion

IL Melting Temperatures. The melting temperatures of the dried ILs, solid at room temperature, were determined by DSC. Only one phase transition was observed in the temperature range evaluated. The melting temperatures, enthalpy and entropy changes at the corresponding melting temperatures, for the crystal to isotropic liquid phase transitions, were, respectively, 311.6 K, 16.7 kJ·mol⁻¹, and 53.6 J·K⁻¹·mol⁻¹ for [C₃mpy][PF₆] (water mole fraction is 0.0038) and 311.2 K, 15.0 kJ·mol⁻¹, and 48.2 J·K⁻¹·mol⁻¹ for [C₃mim][PF₆] (water mole fraction is 0.0012). The corresponding thermograms are presented in the Supporting Information. The melting temperature of [C₃mim][PF₆] obtained in this work is in close agreement with that previously shown in the literature (313.15 K).³ The melting temperatures of the ILs saturated with water are substantially lower than those of the pure ILs, allowing therefore the measurements of [C₃mim][PF₆] to be carried out in the entire temperature range, while for [C₃mpy][PF₆] only for temperatures above 308.15 K the thermophysical properties were evaluated.

IL + Water Mutual Solubilities. The measured solubility data and the respective standard deviations are presented in Table 1. For the studied ILs, the mutual solubilities increase with temperature displaying an upper critical solution temperature behavior. The mole fraction solubility of ILs in water is in the order $\approx 10^{-3}$, but the water solubility in ILs is typically in the order $\approx 10^{-1}$, indicating that they are highly “hygroscopic”, and as previously shown for other hydrophobic ILs.^{25–27} Thus, while the water-rich phase can be considered as an almost pure phase with the IL at infinite dilution, the IL-rich phase presents a significant water content.

Concerning the IL cation influence, it is possible to observe that the hydrophobicity increases from imidazolium- to pyridinium-based ILs, as shown in Figure 1. Comparing with literature data^{25,27} for other ILs with common cations, the IL anion hydrophobicity increases from [PF₆]⁻ to [NTf₂]⁻. Evaluating the influence of both IL cations and anions on the liquid–liquid equilibria with water, it is clear that the major role is played by the IL anion, as previously observed.²⁵

The temperature dependence of the mole fraction solubility can be correlated using eqs 1 and 2 described below.⁵² For the solubility of water in the IL phase, it can be assumed that the process occurs at constant molar enthalpy of solution, and thus,

$$\ln x_w = A + \frac{B}{(T/K)} \quad (1)$$

where x_w is the mole fraction solubility of water in the IL; T is the temperature; and A and B are correlation parameters.

For the solubility of the ILs in water, there is a significant dependence on temperature for the enthalpy of solution and therefore

$$\ln x_{IL} = C + \frac{D}{(T/K)} + E \ln(T/K) \quad (2)$$

where x_{IL} is the mole fraction solubility of the IL in water; T is the temperature; and C , D , and E are correlation parameters.

The correlation constants obtained from the fittings are presented in the Supporting Information. For the IL-rich phase, the proposed correlation shows a relative maximum deviation from experimental mole fraction data of 1 %. Since the solubility of water in all the studied ILs is well above what could be considered infinite dilution, the associated molar thermodynamic functions of solution can not be determined. For the water-rich phase, and because the melting points of both ILs are above 298.15 K, the parameters were calculated in a smaller temperature range from (303.15 to 318.15) K, to avoid the disparities occurring between solid–liquid and liquid–liquid equilibria. The proposed correlation presents a relative maximum deviation from experimental mole fraction data in the order of 1 %.

At the equilibrium state, the chemical potentials of the IL at the aqueous-rich and at the IL-rich phases have to be equivalent, while the electroneutrality of both phases must be obeyed. Quite the opposite of what was observed for the IL-rich phase, the solubility of ILs in the aqueous-rich phase can be considered at infinite dilution, and thus no main solute–solute interactions and/or ion-pairing occurs.⁵³ Therefore, the standard thermodynamic functions of solution, such as standard molar enthalpy ($\Delta_{sol}H_m^0$), molar Gibbs energy ($\Delta_{sol}G_m^0$), and molar entropy ($\Delta_{sol}S_m^0$), were determined for the IL solvation in water. These thermodynamic functions can be calculated according to eqs 3 to 5.⁵⁴

$$\Delta_{sol}G_m^0 = -RT \ln(x_2)_p \quad (3)$$

$$\frac{\Delta_{sol}H_m^0}{RT^2} = \left(\frac{\partial \ln x_2}{\partial T} \right)_p \quad (4)$$

$$\Delta_{sol}S_m^0 = R \left(\frac{\partial \ln x_2}{\partial \ln T} \right)_p \quad (5)$$

where x_2 is the mole fraction solubility of the solute (IL); R is the ideal gas constant; T is the temperature; and the subscript p indicates that the process takes place under constant pressure. The subscript m refers to the molar quantity. The standard molar enthalpy, Gibbs energy, and entropy of solution are reported in Table 2.

The molar enthalpies of solution of the studied ILs in water, at 298.15 K, show that the solubilization of ILs in water is an endothermic process, which is almost independent of the cation nature. Major differences in the enthalpies of solution are observed only for the anion identity (when compared with literature data^{25,27}). This behavior is in agreement with the fact discussed above where the solvation of the anion is the main

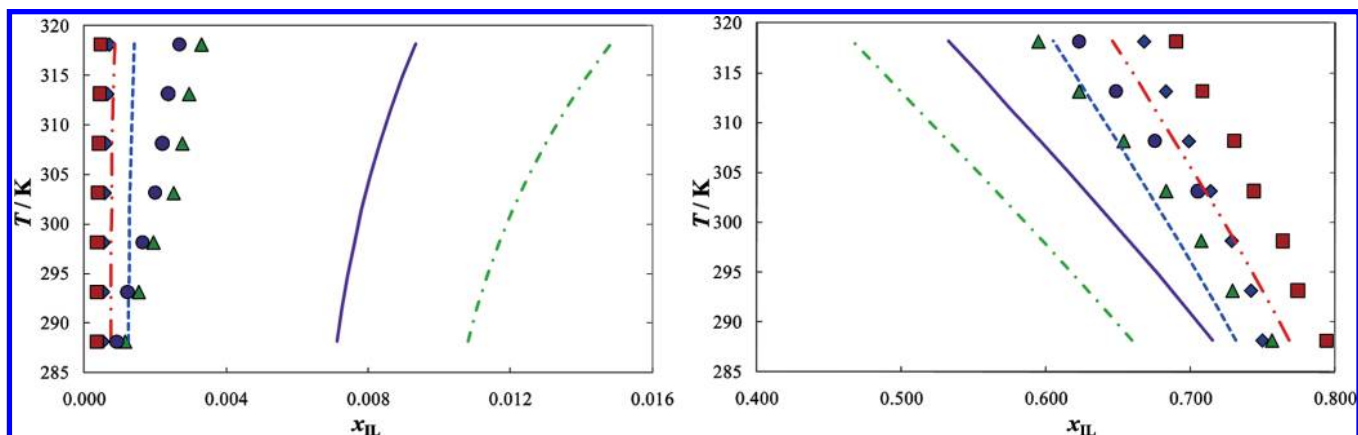


Figure 1. Liquid–liquid phase diagram for water and ILs: \blacklozenge , - - -, $[\text{C}_3\text{mim}][\text{NTf}_2]$;²⁷ \blacksquare , - · - ·, $[\text{C}_3\text{mpy}][\text{NTf}_2]$;²⁵ \blacktriangle , - · - ·, $[\text{C}_3\text{mim}][\text{PF}_6]$; \bullet , - · - ·, $[\text{C}_3\text{mpy}][\text{PF}_6]$. The single symbols and the lines represent, respectively, the experimental data and COSMO-RS prediction results (parameter file BP_TZVP_C2.1_0110).

Table 2. Standard Thermodynamic Molar Properties of Solution of ILs in Water at 298.15 K

IL	$(\Delta_{\text{sol}}H_{\text{m}}^0 \pm \sigma^a)$ kJ·mol ⁻¹	$(\Delta_{\text{sol}}G_{\text{m}}^0 \pm \sigma^a)$ kJ·mol ⁻¹	$(\Delta_{\text{sol}}S_{\text{m}}^0 \pm \sigma^a)$ J·K ⁻¹ ·mol ⁻¹
$[\text{C}_3\text{mim}][\text{PF}_6]$	9.3 ± 1.5	15.460 ± 0.014	-20.7 ± 5.1
$[\text{C}_3\text{mpy}][\text{PF}_6]$	9.1 ± 1.5	15.888 ± 0.043	-22.7 ± 5.2
$[\text{C}_3\text{mim}][\text{NTf}_2]$ ²⁴	5.9 ± 1.5	18.652 ± 0.001	-42.6 ± 5.0
$[\text{C}_3\text{mpy}][\text{NTf}_2]$ ²²	6.5 ± 1.5	19.555 ± 0.016	-43.9 ± 5.1

^a Standard deviation.

issue controlling the solubility of the IL in water. The molar entropies of solution are shown to be negative and little dependent on the cation family, falling within the associated standard deviations. Even so, there are significant differences in the molar entropies of solution when changing the anion while maintaining the cation.^{25,27} More hydrophilic anions are responsible for larger entropic change effects suggesting that the IL dissolution in water is controlled by the anion solvation in the IL-rich phase. The higher (less negative) the entropic change, the higher the solubility of the ILs in water, as can be seen by comparing, for instance, the solubilities for $[\text{C}_3\text{mim}][\text{NTf}_2]$ ²⁷ and $[\text{C}_3\text{mim}][\text{PF}_6]$. $[\text{C}_3\text{mim}][\text{PF}_6]$ is a highly solvated IL in the IL-rich phase, leading to higher (less negative) entropic variations when in equilibrium with the aqueous-rich phase.

Aiming at predicting the ILs–water LLE, the COSMO-RS^{32–36} model was here evaluated. COSMO-RS is a model for predicting the thermodynamic properties of mixtures on the basis of unimolecular quantum chemical calculations for individual species. It merges together the quantum chemical dielectric continuum solvation model, COSMO, with a statistical thermodynamic approach. COSMO-RS calculations for this type of system are detailed elsewhere.^{25,27,37,43}

The results obtained with COSMO-RS are displayed in Figure 1 and show an acceptable qualitative agreement with experimental data. The cation core hydrophobic character increases from $[\text{C}_3\text{mim}]^+$ to $[\text{C}_3\text{mpy}]^+$, observed experimentally, were also observed with COSMO-RS predictions. Moreover, the anion influence through the phase behavior of ILs and water is also well qualitatively predicted. In a previous work,²⁵ using an older version of COSMO-RS (parameter file BP_TZVP_C2.1_0105), some deviations from experimental data were reported, especially regarding the IL anion influence in the liquid–liquid equilibrium. Using the new version of COSMO-RS (parameter file BP_TZVP_C2.1_0110), the prediction of the anion influence is fully consistent with the experimental data, where the anion

$[\text{PF}_6]^-$ presents a smaller liquid–liquid envelope with water when compared to ILs containing the anion $[\text{NTf}_2]^-$. The comparison of both versions of COSMO-RS is depicted in Figure 2. Although improvements in the IL–water phase behavior were observed for the most recent version of COSMO-RS, it should be pointed out that the relative deviations in the experimental values have increased. Nevertheless, the prediction of the correct trend on the influence of IL cations and anions in the liquid–liquid phase behavior using the new version of COSMO-RS is of main importance when the goal is a screening of ILs before experimental measurements. In spite of the quantitative deviations of the COSMO-RS predictions, this method shows to be a useful tool in predicting binary systems behavior, allowing thus an improved choice of the cation and anion composing the IL aiming at designing ILs for specific purposes.

An alternative approach to the estimation of the mutual solubilities of ILs and water is the use of a QSPR correlation previously proposed by us.⁵⁵ Using this correlation, the predicted values for the solubilities of the ILs in water at 303.15 K are $2.48 \cdot 10^{-3}$ and $1.29 \cdot 10^{-3}$ for $[\text{C}_3\text{mim}][\text{PF}_6]$ and $[\text{C}_3\text{mpy}][\text{PF}_6]$, respectively, while the solubilities of water in the ILs at the same temperature are 0.31 and 0.29 (both in mole fraction units). These values when compared with the experimental data have maximum relative deviations of 2.5 % and 5.5 % for the solubility of the ILs in water and water in ILs, respectively.

IL Density Results. The novel experimental density data for both dried and water-saturated ILs are presented in Table 3. Due to the melting temperatures of both dried ILs, densities and viscosities of these “pure” ILs were only measured at temperatures above 318.15 K. For the water-saturated ILs, the presence of a eutectic point allowed the measurements to be carried out in the temperature range between (303.15 and 363.15) K. Figure 3 depicts the density results obtained in this work together with some literature values.^{56,57} For both anions, $[\text{PF}_6]^-$ and $[\text{NTf}_2]^-$, the density values decrease from imidazolium- to pyridinium-based ILs. The molar volumes for a series of ILs with a common anion seem to increase with the effective cation size from imidazolium- to pyridinium-based ILs. Indeed, this tendency is in close agreement with the results previously presented by us⁵⁸ where the molar volumes follow the rank: imidazolium- < pyrrolidinium- < pyridinium- < piperidinium-based ILs. For a given cation, $[\text{C}_3\text{mim}]^+$ or $[\text{C}_3\text{mpy}]^+$, the IL density decreases from $[\text{NTf}_2]^-$ to $[\text{PF}_6]^-$ anions. Therefore, the IL molar volumes also increase with the effective anion size.

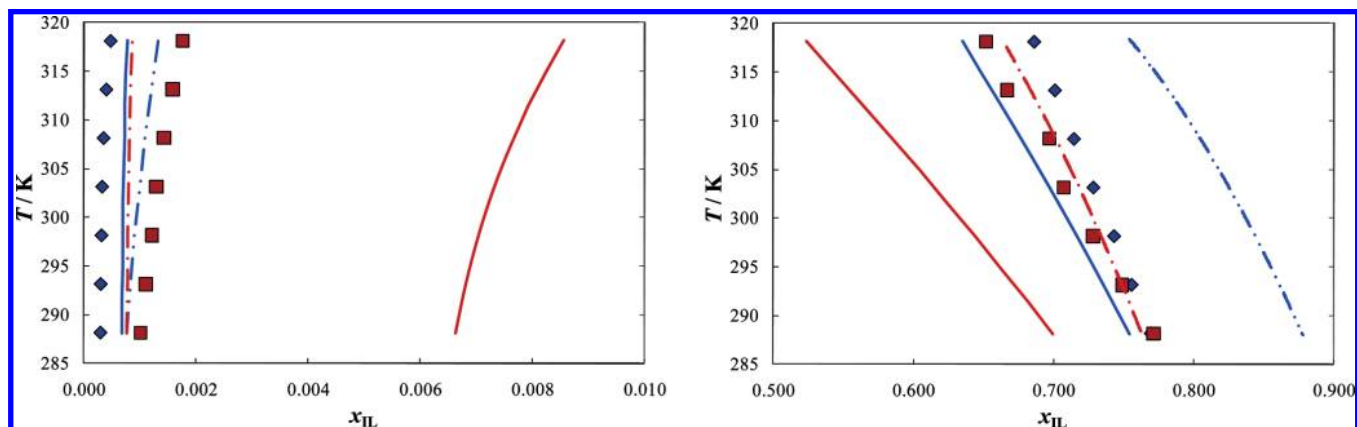


Figure 2. Comparison of COSMO-RS versions for the liquid–liquid phase diagrams of water and ILs: \diamond , $-\cdot\cdot-$, $-$, [C₃mim][NTf₂];²⁷ \blacksquare , $-\cdot\cdot-$, $-$, [C₃mim][PF₆].²⁵ The single symbols, the lines with dots, and the full lines represent, respectively, the experimental data, the COSMO-RS older version (parameter file BP_TZVP_C2.1_0105), and the COSMO-RS new version (parameter file BP_TZVP_C2.1_0110) predictions.

Table 3. Experimental Density Values, ρ , for Pure ILs and (IL + Water) Systems As a Function of Temperature and at 0.1 MPa, Where x_w is the Constant Mole Fraction Solubility of Water in the IL at $T \approx 300$ K

T/K	$\rho/\text{kg}\cdot\text{m}^{-3}$			
	pure		$x_w = (0.306 \pm 0.004^a)$	$x_w = (0.249 \pm 0.006^a)$
	[C ₃ mim][PF ₆]	[C ₃ mpy][PF ₆]	[C ₃ mim][PF ₆]	[C ₃ mpy][PF ₆]
303.15	---	---	1389.2	1362.5
308.15	---	---	1384.7	1358.3
313.15	---	---	1380.2	1354.0
318.15	1397.5	1365.4	1375.7	1349.8
323.15	1393.2	1361.3	1371.3	1345.6
328.15	1389.0	1357.3	1366.9	1341.4
333.15	1384.7	1353.2	1362.5	1337.2
338.15	1380.5	1349.2	1358.1	1333.1
343.15	1376.3	1345.2	1353.8	1328.9
348.15	1372.1	1341.2	1349.4	1324.8
353.15	1367.9	1337.2	1345.1	1320.7
358.15	1363.8	1333.2	1340.8	1316.6
363.15	1359.6	1329.2	1336.5	1312.5

^a Standard deviation.

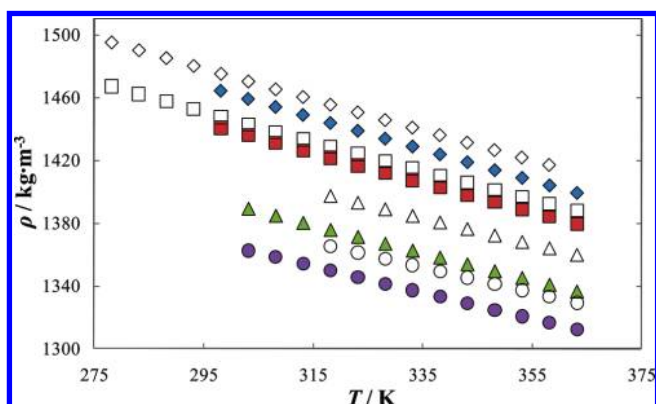


Figure 3. Experimental density as a function of temperature and at 0.1 MPa for the dried ILs (empty symbols) and water-saturated ILs (full symbols): \diamond , \blacksquare , [C₃mim][NTf₂];⁵⁶ \square , \blacksquare , [C₃mpy][NTf₂];⁵⁷ \triangle , \blacktriangle , [C₃mim][PF₆]; \circ , \bullet , [C₃mpy][PF₆].

Figure 3 also presents the results for the water-saturated samples. The presence of water in ILs is shown to decrease their density and has a major impact in ILs that have higher water contents at saturation conditions. However, the trends of the water-saturated ILs are identical to those observed for the dry ILs. At 318.15 K, the density-relative deviations of the water-saturated samples with respect to the pure ILs were in the order of 1.6 % and 1.1 % for [C₃mim][PF₆] and

Table 4. Ionic Volumes, V , Determined with the Gardas and Coutinho Group Contribution Model⁴⁵

species	$V/\text{\AA}^3$
Cations	
1,3-dimethylimidazolium	154 ^a
1,3-dimethylpyridinium	174
Anions	
hexafluorophosphate	107 ^a
additional groups	
–CH ₂	28 ^a

^a Taken from ref 45.

[C₃mpy][PF₆], respectively. These relative deviations, which seem to be temperature independent (note that the water content in both ILs was maintained constant in the entire temperature interval), can be considerably negligible for most application purposes.

To estimate the density data for pure ILs, an extension of the Ye and Shreeve group contribution method proposed previously by Gardas and Coutinho,⁴⁵ and described by eq 6, was used

$$\rho = \frac{M}{NV(a + bT + cp)} \quad (6)$$

where ρ is the density in $\text{kg}\cdot\text{m}^{-3}$; M is the IL molecular weight in $\text{kg}\cdot\text{mol}^{-1}$; N is the Avogadro constant; V is the IL volume in m^3 ; T is the temperature in K; and p is the pressure in MPa. The coefficients a , b , and c , with values of 0.8005 ± 0.0002 , $(6.652 \pm 0.007) \cdot 10^{-4} \text{ K}^{-1}$ and $(-5.919 \pm 0.024) \cdot 10^{-4} \text{ MPa}^{-1}$, respectively, were proposed in a previous work.⁴⁶ The ionic volumes used are reported in Table 4. To obtain the volume parameter for the cation group 1,3-dimethylpyridinium, not previously available, 132 experimental density values taken from the literature (ILs with a similar cation but different anions) were used.^{57,59–62} Figure 4 presents a comparison between the predicted density values based on the group contribution method and the experimental data obtained in this work. The predicted values are in excellent agreement with experimental data, presenting maximum relative deviations of 0.05 % and 0.14 % for [C₃mim][PF₆] and [C₃mpy][PF₆], respectively. This method shows to be highly valuable in the prediction of density data for new ILs where no experimental data are yet available. The complete temperature dependence between the predicted values and those obtained experimentally is depicted in the Supporting Information.

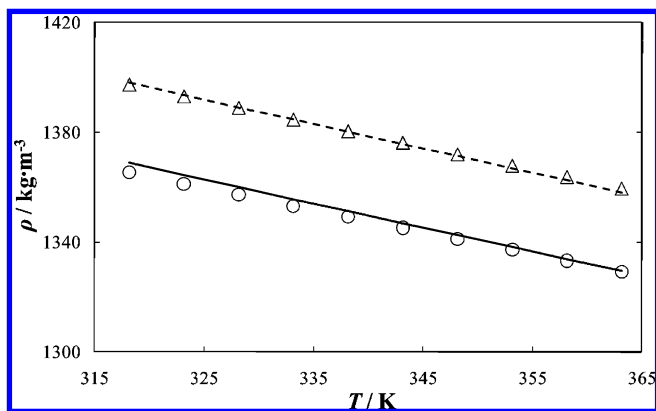


Figure 4. Experimental density as a function of temperature, and at 0.1 MPa, for the dried ILs (symbols) and respective prediction with the Gardas and Coutinho group contribution method⁴⁵ (lines): Δ , ---, [C₃mim][PF₆]; \circ , —, [C₃mpy][PF₆].

Table 5. Thermal Expansion Coefficients, α_p , for Both Pure and Water-Saturated ILs at 318.15 K and 0.1 MPa

T/K	$10^4(\alpha_p \pm \sigma^a)/K^{-1}$			
	pure		$x_w = (0.306 \pm 0.004^a)$	$x_w = (0.249 \pm 0.006^a)$
	[C ₃ mim][PF ₆]	[C ₃ mpy][PF ₆]	[C ₃ mim][PF ₆]	[C ₃ mpy][PF ₆]
318.15	6.023 ± 0.004	5.886 ± 0.004	6.381 ± 0.005	6.174 ± 0.003

^a Standard deviation.

The isobaric thermal expansion coefficients (α_p) associated to each IL were calculated using eq 7

$$\alpha_p = -\frac{1}{\rho} \left(\frac{\partial \rho}{\partial T} \right)_p = - \left(\frac{\partial \ln \rho}{\partial T} \right)_p \quad (7)$$

where ρ is the density in $\text{kg} \cdot \text{m}^{-3}$; T is the temperature in K; and p is the pressure in MPa.

The values of α_p for the ILs here studied are presented in Table 5 and were calculated from the linear relationship between $\ln \rho$ and T using the experimental data gathered in this work. The thermal expansion coefficients were determined at a temperature of 318.15 K due to the high melting temperatures of the ILs under study. For [C₃mim][PF₆] and [C₃mpy][PF₆], the values are $(6.02 \text{ and } 5.89) \cdot 10^{-4} \text{ K}^{-1}$ for the dried samples and $(6.38 \text{ and } 6.17) \cdot 10^{-4} \text{ K}^{-1}$ for the water-saturated samples. The α_p values of both ILs are in close agreement with literature values for related ILs.^{57,63} For both dried and water-saturated, and at a constant temperature, imidazolium-based ILs present higher thermal expansion than their pyridinium-based counterparts. Furthermore, the presence of water increases the values of the isobaric thermal expansion coefficients (α_p).

IL Viscosity Results. The novel viscosity data were determined in the temperature range from (318.15 to 363.15) K for the dried ILs and from (303.15 to 363.15) K for the water-saturated samples. Experimental results are presented in Table 6 and in Figure 5. Also in Figure 5, some literature data^{56,57} are presented for evaluation purposes and to assist the discussion. The viscosity describes the internal resistance of a fluid to a shear stress, and as well-known, ILs present higher viscosities than common volatile organic compounds. Nevertheless, the IL high viscosities are also a direct consequence of their high molecular weights. Since viscosity is mainly dependent on intermolecular interactions (H-bonding, dispersive and Coulombic interactions), an increase in temperature will substantially decrease the intensity of H-bonding interactions, and therefore

Table 6. Experimental Viscosity Values, η , for Pure ILs and (IL + Water) Systems As a Function of Temperature and at 0.1 MPa, Where x_w is the Constant Mole Fraction Solubility of Water in the IL at $T \approx 300 \text{ K}$

T/K	$\eta/\text{mPa} \cdot \text{s}$			
	dried		$x_w = (0.306 \pm 0.004^a)$	$x_w = (0.249 \pm 0.006^a)$
	[C ₃ mim][PF ₆]	[C ₃ mpy][PF ₆]	[C ₃ mim][PF ₆]	[C ₃ mpy][PF ₆]
303.15	---	---	39.408	73.388
308.15	---	---	32.254	57.548
313.15	---	---	26.844	45.980
318.15	85.006	132.870	22.612	37.356
323.15	68.178	102.170	19.285	30.806
328.15	55.458	79.968	16.581	25.755
333.15	45.700	63.669	14.386	21.759
338.15	38.092	51.520	12.612	18.602
343.15	32.099	42.287	11.134	16.037
348.15	27.321	35.160	9.905	13.976
353.15	23.469	29.579	8.874	12.277
358.15	20.337	25.148	7.983	10.861
363.15	17.771	21.594	7.228	9.677

^a Standard deviation.

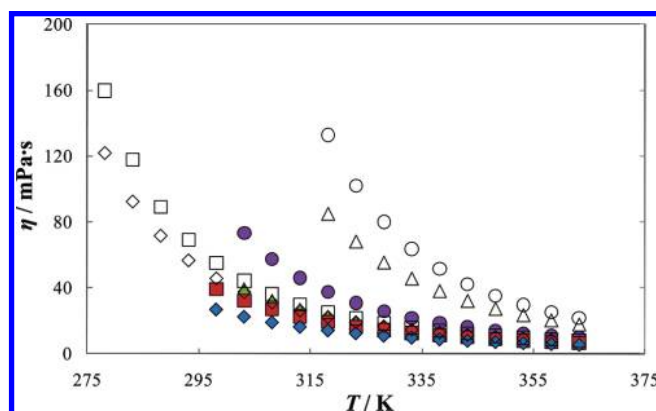


Figure 5. Experimental viscosity as a function of temperature, and at 0.1 MPa, for the dried ILs (empty symbols) and water-saturated ILs (full symbols): \diamond , \blacklozenge , [C₃mim][NTf₂];⁵⁶ \square , \blacksquare , [C₃mpy][NTf₂];⁵⁷ Δ , \blacktriangle , [C₃mim][PF₆]; \circ , \bullet , [C₃mpy][PF₆].

the viscosity largely decreases. While densities decrease from imidazolium- to pyridinium-based ILs, the viscosities decrease from pyridinium- to imidazolium-based ILs. This is in agreement with the results of Crosthwaite et al.⁶⁴ that showed that pyridinium-based salts are generally more viscous than the equivalent imidazolium salts. In addition, for a common cation, [C₃mim]⁺, the viscosities decrease for ILs based on [PF₆]⁻ to [NTf₂]⁻. From the inspection of Figure 5, the IL viscosities seem to be more dependent on the anion than on the IL cation nature.

As for density values, the presence of water in ILs decreases the IL viscosity and has a major impact on those which are less hydrophobic. Relative deviations of the water-saturated samples to the pure ILs, at 318.15 K, were 73 % and 72 % for [C₃mim][PF₆] and [C₃mpy][PF₆], respectively. The influence of the water content in the viscosity is much more pronounced than in density. However, as temperature increases, the effect of water becomes less important because of the weakening of the H-bonding interactions between ILs and water.

The experimental viscosity data here measured were correlated using the Vogel–Tammann–Fulcher model described in eq 8

$$\ln \eta = A_\eta + \frac{B_\eta}{(T - T_{0\eta})} \quad (8)$$

Table 7. Correlation Parameters A_η and B_η Obtained from the Vogel–Tammann–Fulcher Correlation⁶⁵ Applied to Experimental Data for Dried and Water-Saturated ILs

ILs	A_η		B_η/K		$T_{0\eta}/K$	
	dried	saturated	dried	saturated	dried	saturated
[C ₃ mim][PF ₆]	-9.363	-9.426	1055.34	982.29	165.06	143.98
[C ₃ mpy][PF ₆]	-10.009	-10.021	1220.37	1174.10		

where η is viscosity in Pa·s; T is temperature in K; and A_η , B_η , and $T_{0\eta}$ are adjustable parameters. In Table 7, the parameters A_η , B_η , and $T_{0\eta}$ determined from the correlation of the experimental data for both dried and water-saturated ILs are presented. Figure 6 displays the experimental data and respective comparison with the proposed correlation. The average relative deviations between the correlated values and experimental data are 0.20 % for [C₃mim][PF₆] and 0.70 % for [C₃mpy][PF₆] for pure ILs and 0.72 % for [C₃mim][PF₆] and 1.24 % for [C₃mpy][PF₆] for water-saturated ILs. The Vogel–Tammann–Fulcher method provides a good description of the viscosity dependence on temperature for both ILs and for both pure and water-saturated samples.

The prediction of viscosities for the studied ILs was also carried out based on the group contribution method proposed by Gardas and Coutinho⁶⁵ which makes use of the Vogel–Tammann–Fulcher model described in eq 8. A_η and B_η are obtained by a group contribution method according to

$$A_\eta = \sum_{i=1}^k n_i a_{i,\eta} \quad (9)$$

$$B_\eta = \sum_{i=1}^k n_i b_{i,\eta} \quad (10)$$

where n_i is the number of groups of type i and k is the total number of different groups in the molecule. Parameters $a_{i\eta}$ and $b_{i\eta}$ are provided in Table 8 for the studied ILs. Some of these values were previously estimated and were taken from literature.⁶⁵ However, a new group (cation 1,3-dimethylpyridinium) is here proposed. This new group was obtained by the correlation of the experimental viscosity values gathered in this work together with experimental data reported in literature.^{57,59–62,64} For dried samples, the $T_{0\eta}$ of 165.06 K previously proposed was used.⁶⁵ The averages of the absolute relative

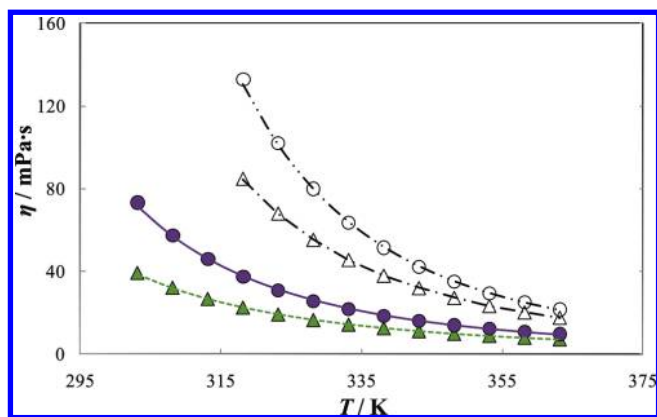


Figure 6. Experimental viscosity as a function of temperature, and at 0.1 MPa, for the dried ILs (empty symbols), water-saturated ILs (full symbols), and respective correlations using the Vogel–Tammann–Fulcher⁶⁵ method (lines): Δ , $- \cdot -$, $- - -$, [C₃mim][PF₆]; \circ , $- \cdot - \cdot -$, $- -$, [C₃mpy][PF₆].

Table 8. Group Contribution Parameters $a_{i,\eta}$ and $b_{i,\eta}$ for the Group Contribution Method Proposed by Gardas and Coutinho⁶⁵ Based on the Vogel–Tammann–Fulcher Correlation

species	$a_{i,\eta}$	$b_{i,\eta}/K$
Cations		
1,3-dimethylimidazolium	-7.271 ^a	510.51 ^a
1,3-dimethylpyridinium	-7.581	605.98
Anions		
hexafluorophosphate	-1.834 ^a	433.14 ^a
Additional Groups		
-CH ₂	-7.528·10 ⁻² ^a	40.92 ^a

^a Taken from ref 64.

Table 9. Comparison between the Correlated and Predicted Parameters A_η and B_η from the Vogel–Tammann–Fulcher Correlation Applied to the Experimental Data and from the Group Contribution Method Proposed by Gardas and Coutinho⁶⁵

ILs	A_η		B_η/K	
	predicted	correlated	predicted	correlated
[C ₃ mim][PF ₆]	-9.256	-9.363	1025.49	1055.34
[C ₃ mpy][PF ₆]	-9.566	-10.009	1120.96	1220.37

deviations between the predictions and the experimental data are 6.7 % and 13.9 % for pure ILs [C₃mim][PF₆] and [C₃mpy][PF₆], respectively. The relative deviations between the experimental data and those predicted for the entire temperature interval are shown in the Supporting Information. In Table 9, a comparison between predicted (using eqs 8 to 10) and correlated (applying only eq 8 to the experimental data) parameters A_η and B_η is presented.

Conclusions

New data for physical properties, such as melting temperatures, densities and viscosities, and mutual solubilities with water, of ILs based on imidazolium and pyridinium cations in combination with the hexafluorophosphate anion were here determined.

The mutual solubilities show that the hydrophobicity of the cation family increases from imidazolium- to pyridinium-based ILs. The standard molar enthalpies of solution of ILs in water have shown to be insignificantly dependent on the cation core, while the major contributions to the solubility are related to the IL anion identity, arising from considerable enthalpic and entropic solvation differentiations. The COSMO-RS proved to be valuable in the prediction of the behavior of water and IL binary systems. This predictive method provided an adequate semiquantitative description of the data in good qualitative agreement with the experimental results.

Experimental densities decrease from imidazolium- to pyridinium-based ILs, while experimental viscosities show the opposite behavior. Both density and viscosity of ILs decrease in the presence of water, yet the effect of water content on the IL viscosities is particularly remarkable.

Acknowledgment

The authors thank financial support from Fundação para a Ciência e a Tecnologia (Projects PTDC/EQU-FTT/65252/2006 and REEQ/515/CTM/2005) and Postdoctoral grant SFRH/BPD/41781/2007 of MGF. The authors also thank Sandra Magina for the operation with the Diamond DSC PerkinElmer.

Supporting Information Available:

Additional experimental details and Figures S1 to S5 and Tables S1 and S2. This material is available free of charge via the Internet at <http://pubs.acs.org>.

Literature Cited

- Koel, M. *Ionic Liquids in Chemical Analysis*; CRC Press: New York, 2009.
- Ventura, S. P. M.; Gonçalves, A. M. M.; Gonçalves, F.; Coutinho, J. A. P. Assessing the Toxicity on [C₃mim][Tf₂N] to Aquatic Organisms of Different Trophic Levels. *Aquat. Toxicol.* **2010**, *96*, 290–297.
- Ngo, H. L.; LeCompte, K.; Hargens, L.; McEwen, A. B. Thermal Properties of Imidazolium Ionic Liquids. *Thermochim. Acta* **2000**, *357–358*, 97–102.
- Muhammad, A.; Mutalib, M. I. A.; Wilfred, C. D.; Murugesan, T.; Shafeeq, A. Thermophysical Properties of 1-Hexyl-3-methyl Imidazolium based Ionic Liquids with Tetrafluoroborate, Hexafluorophosphate and Bis(trifluoromethylsulfonyl)imide Anions. *J. Chem. Thermodyn.* **2008**, *40*, 1433–1438.
- Huddleston, J. G.; Visser, A. E.; Reichert, W. M.; Willauer, H. D.; Broker, G. A.; Rogers, R. D. Characterization and Comparison of Hydrophilic and Hydrophobic Room Temperature Ionic Liquids Incorporating the Imidazolium Cation. *Green Chem.* **2001**, *3*, 156–164.
- Wasserscheid, P.; Welton, T. *Ionic Liquids in Synthesis*; Wiley-VCH: Weinheim, 2003.
- Plechkova, N. V.; Seddon, K. R. Applications of Ionic Liquids in the Chemical Industry. *Chem. Soc. Rev.* **2008**, *37*, 123–150.
- Visser, A. E.; Holbrey, J. D.; Rogers, R. D. Hydrophobic Ionic Liquids Incorporating N-alkylisquinolinium Cations and their Utilization in Liquid-liquid Separations. *Chem. Commun.* **2001**, 2484–2485.
- Matsumoto, M.; Mochiduki, K.; Fukunishi, K.; Kondo, K. Extraction of Organic Acids Using Imidazolium-based Ionic Liquids and their Toxicity to Lactobacillus Rhamnosus. *Sep. Purif. Technol.* **2004**, *40*, 97–101.
- Khachatryan, K. S.; Smirnova, S. V.; Torocheshnikova, I. V.; Shvedene, N. V.; Formanovsky, A. A.; Pletnev, I. V. Solvent Extraction and Extraction-Voltammetric Determination of Phenols Using Room Temperature Ionic Liquid. *Anal. Bioanal. Chem.* **2005**, *381*, 464–470.
- Vidal, S. T. M.; Correlá, M. J. N.; Marques, M. M.; Ismael, M. R.; Reis, M. T. A. Studies on the Use of Ionic Liquids as Potential Extractants of Phenolic Compounds and Metal Ions. *Sep. Sci. Technol.* **2004**, *39*, 2155–2169.
- Fan, J.; Fan, Y.; Pei, Y.; Wu, K.; Wang, J.; Fan, M. Solvent Extraction of Selected Endocrinedisrupting Phenols Using Ionic Liquids. *Sep. Purif. Technol.* **2008**, *61*, 324–331.
- Smirnova, S. V.; Torocheshnikova, I. V.; Formanovsky, A. A.; Pletnev, I. V. Solvent Extraction of Amino Acids into Room-Temperature Ionic Liquid with Dicyclohexano-18-crown-6. *Anal. Bioanal. Chem.* **2004**, *378*, 1369–1375.
- Wang, J.; Pei, Y.; Zhao, Y.; Hu, Z. Recovery of Amino Acids by Imidazolium Based Ionic Liquids from Aqueous Media. *Green Chem.* **2005**, *7*, 196–202.
- Soto, A.; Arce, A.; Khoshkbarchi, M. K. Partitioning of Antibiotics in a Two-liquid Phase System Formed by Water and a Room Temperature Ionic Liquid. *Sep. Purif. Technol.* **2005**, *44*, 242–246.
- Vijayaraghavan, R.; Vedaraman, N.; Surianarayanan, M.; MacFarlane, D. R. Extraction and Recovery of Azo Dyes into an Ionic Liquid. *Talanta* **2006**, *69*, 1059–1062.
- Li, C.; Xin, B.; Xu, W.; Zhang, Q. Study on the Extraction of Dyes into a Room-Temperature Ionic Liquid and their Mechanisms. *J. Chem. Technol. Biotechnol.* **2007**, *82*, 196–204.
- Jork, C.; Seller, M.; Beste, Y. A.; Arit, W. Influence of Ionic Liquids on the Phase Behavior of Aqueous Azeotropic Systems. *J. Chem. Eng. Data* **2004**, *49*, 852–857.
- McFarlane, J.; Ridenour, W. B.; Luo, H.; Hunt, R. D.; DePaoli, D. W.; Ren, R. X. Room Temperature Ionic Liquids for Separating Organics from Produced Water. *Sep. Sci. Technol.* **2005**, *40*, 1245–1265.
- Anthony, J. L.; Maginn, E. J.; Brennecke, J. F. Solution Thermodynamics of Imidazolium-Based Ionic Liquids and Water. *J. Phys. Chem. B* **2001**, *105*, 10942–10949.
- Crosthwaite, J. M.; Aki, S.; Maginn, E. J.; Brennecke, J. F. Liquid Phase Behavior of Imidazolium-Based Ionic Liquids with Alcohols. *J. Phys. Chem. B* **2004**, *108*, 5113–5119.
- Rebello, L. P. N.; Najdanovic-Visak, V.; Visak, Z. P.; da Ponte, M. N.; Szydłowski, J.; Cerdeira, C. A.; Troncoso, J.; Romani, L.; Esperanca, J.; Guedes, H. J. R.; de Sousa, H. C. A Detailed Thermodynamic Analysis of [C₄mim][BF₄]⁺ Water as a Case Study to Model Ionic Liquid Aqueous Solutions. *Green Chem.* **2004**, *6*, 369–381.
- Wong, D. S. H.; Chen, J. P.; Chang, J. M.; Chou, C. H. Phase Equilibria of Water and Ionic Liquids [emim][PF₆] and [bmim][PF₆]. *Fluid Phase Equilib.* **2002**, *194*, 1089–1095.
- Chapeaux, A.; Simoni, L. D.; Stadtherr, M. A.; Brennecke, J. F. Liquid Phase Behavior of Ionic Liquids with Water and 1-Octanol and Modeling of 1-Octanol/Water Partition Coefficients. *J. Chem. Eng. Data* **2007**, *52*, 2462–2467.
- Freire, M. G.; Neves, C. M. S. S.; Carvalho, P. J.; Gardas, R. L.; Fernandes, A. M.; Marrucho, I. M.; Santos, L. M. N. B. F.; Coutinho, J. A. P. Mutual Solubilities of Water and Hydrophobic Ionic Liquids. *J. Phys. Chem. B* **2007**, *111*, 13082–13089.
- Freire, M. G.; Santos, L. M. N. B. F.; Fernandes, A. M.; Coutinho, J. A. P.; Marrucho, I. M. An Overview of the Mutual Solubilities of Water-imidazolium-based Ionic Liquids Systems. *Fluid Phase Equilib.* **2007**, *261*, 449–454.
- Freire, M. G.; Carvalho, P. J.; Gardas, R. L.; Marrucho, I. M.; Santos, L. M. N. B. F.; Coutinho, J. A. P. Mutual Solubilities of Water and the [C_nmim][Tf₂N] Hydrophobic Ionic Liquids. *J. Phys. Chem. B* **2008**, *112*, 1604–1610.
- Freire, M. G.; Carvalho, P. J.; Gardas, R. L.; Santos, L. M. N. B. F.; Marrucho, I. M.; Coutinho, J. A. P. Solubility of Water in Tetradecyltrihexylphosphonium-Based Ionic Liquids. *J. Chem. Eng. Data* **2008**, *53*, 2378–2382.
- Freire, M. G.; Carvalho, P. J.; Silva, A. M. S.; Santos, L. M. N. B. F.; Rebello, L. P. N.; Marrucho, I. M.; Coutinho, J. A. P. Ion Specific Effects on the Mutual Solubilities of Water and Hydrophobic Ionic Liquids. *J. Phys. Chem. B* **2009**, *113*, 202–211.
- Tomé, L. I. N.; Varanda, F. R.; Freire, M. G.; Marrucho, I. M.; Coutinho, J. A. P. Towards an Understanding of the Mutual Solubilities of Water and Hydrophobic Ionic Liquids in the Presence of Salts: The Anion Effect. *J. Phys. Chem. B* **2009**, *113*, 2815–2825.
- Freire, M. G.; Neves, C. M. S. S.; Marrucho, I. M.; Coutinho, J. A. P.; Fernandes, A. M. Hydrolysis of Tetrafluoroborate and Hexafluorophosphate Counter Ions in Imidazolium-Based Ionic Liquids. *J. Phys. Chem. A* **2010**, *114*, 3744–3749.
- Klamt, A.; Schuurmann, G. J. COSMO: a New Approach to Dielectric Screening in Solvents with Explicit Expressions for the Screening Energy and its Gradient. *Chem. Soc., Perkin Trans. II* **1993**, *2*, 799–805.
- Klamt, A. Conductor-like Screening Model for Real Solvents: A New Approach to the Quantitative Calculation of Solvation Phenomena. *J. Phys. Chem.* **1995**, *99*, 2224–2235.
- Klamt, A.; Eckert, F. COSMO-RS: a Novel and Efficient Method for the a priori Prediction of Thermophysical data of liquids. *Fluid Phase Equilib.* **2000**, *172*, 43–72.
- Klamt, A. *COSMO-RS from Quantum Chemistry to Fluid Phase Thermodynamics and Drug Design*; Elsevier: Amsterdam, 2005.
- Eckert, F.; Klamt, A. Fast Solvent Screening via Quantum Chemistry: COSMO-RS Approach. *AIChE J.* **2002**, *48*, 369–385.
- Freire, M. G.; Santos, L. M. N. B. F.; Marrucho, I. M.; Coutinho, J. A. P. Evaluation of COSMO-RS for the Prediction of LLE and VLE of Alcohols + Ionic Liquids. *Fluid Phase Equilib.* **2007**, *255*, 167–178.
- Marsh, K. N.; Deev, A. V.; Wu, A. C.-T.; Tran, E.; Klamt, A. Room Temperature Ionic Liquids as Replacements for Conventional Solvents - A review. *Korean J. Chem. Eng.* **2002**, *19*, 357–362.
- Domańska, U.; Pobudkowska, A.; Eckert, F. Liquid-liquid Equilibria in the Binary Systems (1,3-Dimethylimidazolium, or 1-Butyl-3-methylimidazolium Methylsulfate + Hydrocarbons). *Green Chem.* **2006**, *8*, 268–276.
- Domańska, U.; Pobudkowska, A.; Eckert, F. (Liquid + Liquid) Phase Equilibria of 1-Alkyl-3-methylimidazolium Methylsulfate with Alcohols, or Ethers, or Ketones. *J. Chem. Thermodyn.* **2006**, *38*, 685–695.
- Sahandzhiyeva, K.; Tuma, D.; Breyer, S.; Kamps, A. P.-S.; Maurer, G. G. Liquid-liquid Equilibrium in Mixtures of the Ionic Liquid 1-*n*-Butyl-3-methylimidazolium Hexafluorophosphate and an Alkanol. *J. Chem. Eng. Data* **2006**, *51*, 1516–1525.
- Wu, C.-T.; Marsh, K. N.; Deev, A. V.; Boxall, J. A. Liquid-liquid Equilibria of Room-Temperature Ionic Liquids and Butan-1-ol. *J. Chem. Eng. Data* **2003**, *48*, 486–491.
- Freire, M. G.; Ventura, S. P. M.; Santos, L. M. N. B. F.; Marrucho, I. M.; Coutinho, J. A. P. Evaluation of COSMO-RS for the Prediction of LLE and VLE of Water and Ionic Liquids Binary Systems. *Fluid Phase Equilib.* **2008**, *268*, 74–84.
- Tomé, L. I. N.; Carvalho, P. J.; Freire, M. G.; Marrucho, I. M.; Fonseca, I. M. A.; Ferreira, A. G. M.; Coutinho, J. A. P.; Gardas, R. L. Measurements and Correlation of High-Pressure Densities of Imidazolium-Based Ionic Liquids. *J. Chem. Eng. Data* **2008**, *53*, 1914–1921.
- Gardas, R. L.; Coutinho, J. A. P. Extension of the Ye and Shreeve Group Contribution Method for Density Estimation of Ionic Liquids in a Wide Range of Temperatures and Pressures. *Fluid Phase Equilib.* **2008**, *263*, 26–32.
- Carvalho, P. J.; Regueira, T.; Santos, L. M. N. B. F.; Fernandez, J.; Coutinho, J. A. P. Effect of Water on the Viscosities and Densities of 1-Butyl-3-methylimidazolium Dicyanamide and 1-Butyl-3-methylimidazolium Tricyanomethane at Atmospheric Pressure. *J. Chem. Eng. Data* **2010**, *55*, 645–652.

- (47) Fredlake, C. P.; Crosthwaite, J. M.; Hert, D. G.; Aki, S. N. V. K.; Brennecke, J. F. Thermophysical properties of imidazolium-based ionic liquids. *J. Chem. Eng. Data* **2004**, *49*, 954–964.
- (48) Gardas, R. L.; Freire, M. G.; Carvalho, P. J.; Marrucho, I. M.; Fonseca, I. M. A.; Ferreira, A. G. M.; Coutinho, J. A. P. $P\rho T$ Measurements of Imidazolium-Based Ionic Liquids. *J. Chem. Eng. Data* **2007**, *52*, 1881–1888.
- (49) Ahlrichs, R.; Bär, M.; Häser, M.; Horn, H.; Kölmel, C. Electronic Structure Calculations on Workstation Computers: The program system turbomole. *Chem. Phys. Lett.* **1989**, *162*, 165–169.
- (50) Schäfer, A.; Klamt, A.; Sattel, D.; Lohrenz, J. C. W.; Eckert, F. COSMO Implementation in TURBOMOLE: Extension of an Efficient Quantum Chemical Code Towards Liquid Systems. *Phys. Chem. Chem. Phys.* **2000**, *2*, 2187–2193.
- (51) Schäfer, A.; Huber, C.; Ahlrichs, R. Fully Optimized Contracted Gaussian Basis Sets of Triple Zeta Valence Quality for Atoms Li to Kr. *J. Chem. Phys.* **1994**, *100*, 5829–5835.
- (52) Tsionopoulos, C. Thermodynamic analysis of the mutual solubilities of normal alkanes and water. *Fluid Phase Equilib.* **1999**, *156*, 21–33.
- (53) Canongia Lopes, J. N. A.; Pádua, A. A. H. Nanostructural Organization in Ionic Liquids. *J. Phys. Chem. B* **2006**, *110*, 3330–3335.
- (54) Adkins, C. J. *Equilibrium Thermodynamics*; McGraw Hill: London, 1968.
- (55) Freire, M. G.; Neves, C. M. S. S.; Ventura, S. P. M.; Pratas, M. J.; Marrucho, I. M.; Oliveira, J.; Coutinho, J. A. P.; Fernandes, A. M. Solubility of Non-aromatic Ionic Liquids in Water and Correlation Using a QSPR Approach. *Fluid Phase Equilib.* **2010**, *294*, 234–240.
- (56) Tariq, M.; Carvalho, P. J.; Coutinho, J. A. P.; Marrucho, I. M.; Canongia Lopes, J. N.; Rebelo, L. P. N. Viscosity of (C_2 – C_{14}) 1-Alkyl-3-methylimidazolium Bis(trifluoromethylsulfonyl)amide Ionic Liquids in an Extended Temperature Range. *Fluid Phase Equilib.* **2010**, submitted.
- (57) Oliveira, F. S.; Freire, M. G.; Carvalho, P. J.; Coutinho, J. A. P.; Lopes, J. N. C.; Rebelo, L. P. N.; Marrucho, I. M. Structural and Positional Isomerism Influence in the Physical Properties of Pyridinium NTf₂-Based Ionic Liquids: Pure and Water-Saturated Mixtures. *J. Chem. Eng. Data* **2010**, DOI: 10.1021/je100377k.
- (58) Gardas, R. L.; Costa, H. F.; Freire, M. G.; Carvalho, P. J.; Marrucho, I. M.; Fonseca, I. M. A.; Ferreira, A. G. M.; Coutinho, J. A. P. Densities and Derived Thermodynamic Properties of Imidazolium-, Pyridinium-, Pyrrolidinium-, and Piperidinium-Based Ionic Liquids. *J. Chem. Eng. Data* **2008**, *53*, 805–811.
- (59) Bandrés, I.; Giner, B.; Artigas, H.; Lafuente, C.; Royo, F. M. Thermophysical Properties of N-Octyl-3-methylpyridinium Tetrafluoroborate. *J. Chem. Eng. Data* **2009**, *54*, 236–240.
- (60) Bandrés, I.; Giner, B.; Gascón, I.; Castro, M.; Lafuente, C. Physico-chemical Characterization of n-Butyl-3-methylpyridinium Dicyanamide Ionic Liquid. *J. Phys. Chem. B* **2008**, *112*, 12461–12467.
- (61) Bandrés, I.; Giner, B.; Artigas, H.; Royo, F. M.; Lafuente, C. Thermophysical Comparative Study of Two Isomeric Pyridinium-Based Ionic Liquids. *J. Phys. Chem. B* **2008**, *112*, 3077–3084.
- (62) Sánchez, L. G.; Espel, J. R.; Onink, F.; Meindersma, G. W.; Haan, A. B. Density, Viscosity, and Surface Tension of Synthesis Grade Imidazolium, Pyridinium, and Pyrrolidinium Based Room Temperature Ionic Liquids. *J. Chem. Eng. Data* **2009**, *54*, 2803–2812.
- (63) Jacquemin, J.; Husson, P.; Padua, A. A. H.; Majer, V. Density and Viscosity of Several Pure and Water-Saturated Ionic Liquids. *Green Chem.* **2005**, *8*, 172–180.
- (64) Crosthwaite, J. M.; Muldoon, M. J.; Dixon, J. K.; Anderson, J. L.; Brennecke, J. F. Phase Transition and Decomposition Temperatures, Heat Capacities and Viscosities of Pyridinium Ionic Liquids. *J. Chem. Thermodyn.* **2005**, *37*, 559–568.
- (65) Gardas, R. L.; Coutinho, J. A. P. Group Contribution Methods for the Prediction of Thermophysical and Transport Properties of Ionic Liquids. *AIChE J.* **2009**, *55*, 1274–1290.

Received for review June 9, 2010. Accepted July 27, 2010.

JE100638G